Electronic Supplementary Material (ESI) for Journal of Materials Chemistry C.

Compact and Ultrathin Multi-elements Oxide Films Grown by Temperature-Controlled Deposition and Their Surface-Potential Based Transistors Theoretical Simulation

Jiahui Liu, Zunxian Yang*, Shimin Lin, Kang Zheng, Yuliang Ye, Bingqing Ye, Zhipeng Gong, Yinglin Qiu, Lei Xu, Tailiang Guo, Sheng Xu

National & Local United Engineering Laboratory of Flat Panel Display Technology, Fuzhou University, Fuzhou 350116, P. R. China.

Supporting Information

Captions

Figure S1 (a-e) Cross-section height profile of film deposited (using Zinc acetate dihydrate precursor) at the heating substrate in the range of 125℃-390℃. **(f)** Average diameter plot of the films corresponding **(a-e)** samples.

Figure S2 TGA curve of Indium acetate anhydrous and Magnesium acetate tetrahydrate powder respectively that tested under air at a scan rate of 10℃/min.

Figure S3 3D **(a)** and 2D **(b)** morphology image of the IMZO films deposited at the heating substrate in the range of 125℃-395℃.

Figure S4 SEM image of patterned IMZO films deposited at the heating substrate at **(a)** 125℃ (Inset: high-magnification of sample in **(a)**), **(b-c)** 395℃.

Figure S5 Morphology images of ZnO, MZO, MgO, ZnO-1, IZO and IMZO film: **(a)** large-scale film (scale bars: 500 μm), **(b)** patterned film (scale bars: 200 μm).

Figure S6 AFM images of films including the height and line-scan profile: **(a)** ZnO, **(b)** MgO, **(c)** MZO, **(d)** ZnO-1, **(e)** IZO, **(f)** IMZO (scale bar: 200 nm).

Figure S7 EDS analysis of the films corresponding to Figure 3c samples: **(a)** ZnO, **(b)** MgO, **(c)** MZO, **(d)** ZnO-1, **(e)** IZO, **(f)** IMZO.

Figure S8 Cross-section height profile of ZnO, MZO, ZnO-1, IZO and IMZO films corresponding to **Figure 3 (e-i)** samples respectively.

Table S1 Performance parameters of experimental data (white bar) and simulation model (blue bar) for ZnO, MZO, ZnO-1, IZO and IMZO TFTs. The channel length/width of transistors was kept 40 μm/200 μm.

Table S2 Comparisons of electrical parameters of reported metal oxide based TFTs.

Figure S9 Transfer (V_{ds}=5 V) characteristics of metal oxide TFTs corresponding to **Figure 5 (a-e)** samples. The black dashed and green lines indicate the slopes for the calculation of field-effect mobility and effective mobility respectively.

Figure S10 (a) Field effect mobility (μ_{FE}), **(b)** Threshold voltage (V_{th}) and **(c)** Subshreshold swing (SS) distribution for 24 nm-ZnO, 24 nm-MZO, 5 nm-ZnO-1, 5 nm-IZO and 5 nm-IMZO TFTs respectively. (V_{ds}=5 V and V_{gs}=-40 V-60 V).

Table S3 Parameters for simulations of ZnO TFTs with different ratio of In or Mg contents. The channel length/width of transistors was kept 40 μm /200 μm.

Table S4 Performance parameters of experimental data (white bar) and simulation model (blue bar) for ZnO and IMZO TFTs with different thickness. The channel length/width of transistors was kept 40 μm /200□ μm.

Table S5 Parameters for simulation of ZnO and IMZO TFTs with different thickness. The channel length/width of transistors was kept 40 μm /200 μm.

Figure S11 SEM image of different thickness of patterned ZnO films: **(a)** 10 nm, **(b)** 21 nm, **(c)** 24 nm, **(d)** 35 nm. The insets show the cross-section height profile of corresponding ZnO films.

Figure S12 SEM image of different thickness of patterned IMZO films: **(a)** 5 nm, **(b)** 6 nm, **(c)** 7 nm, **(d)** 8 nm. The insets show the cross-section height profile of corresponding IMZO films.

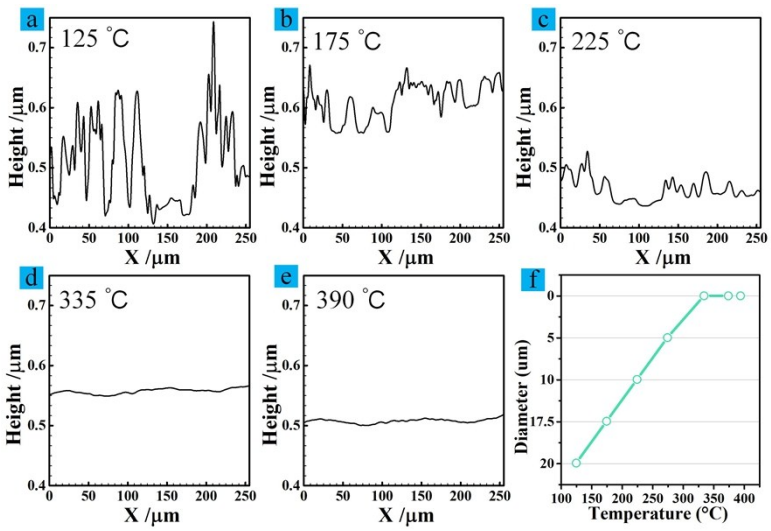
a
125 ˚C
b
175 ˚C
c
225 ˚C
d
335 ˚C
e
390 ˚C
f
Height /μm
X /μm
Diameter (um)
Temperature (°C)

Figure S1

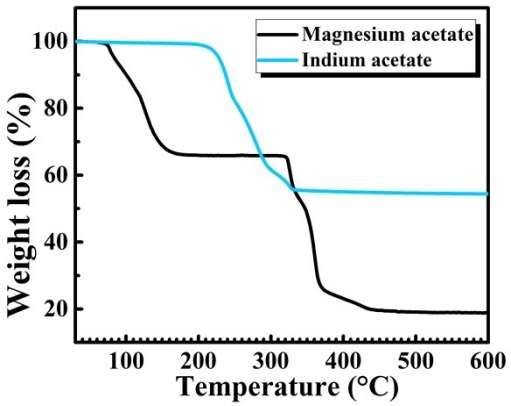
Magnesium acetate
Indium acetate
Weight loss (%)
100
80
60
40
20
100
200
300
400
500
600
Temperature (°C)

Figure S2

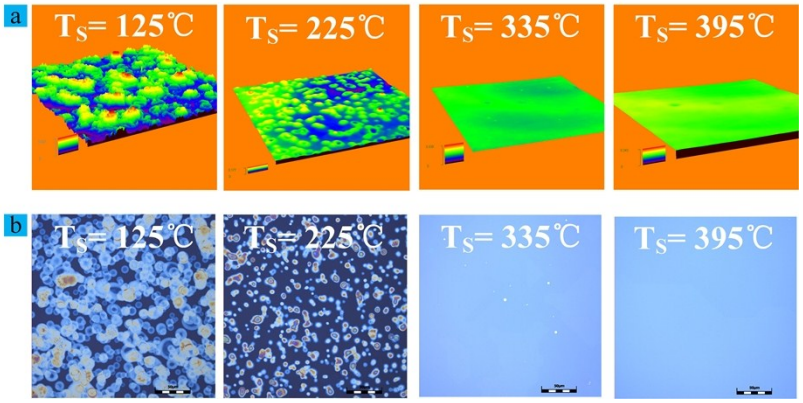

Figure S3

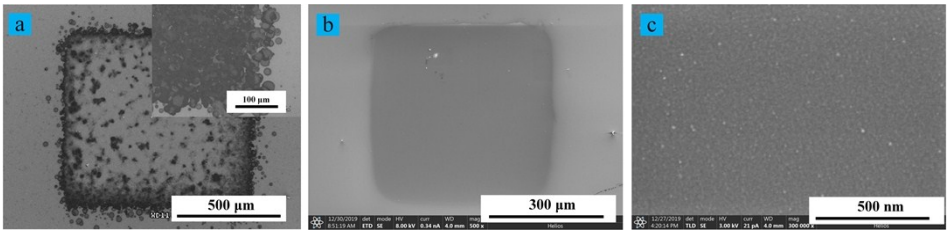

Figure S4

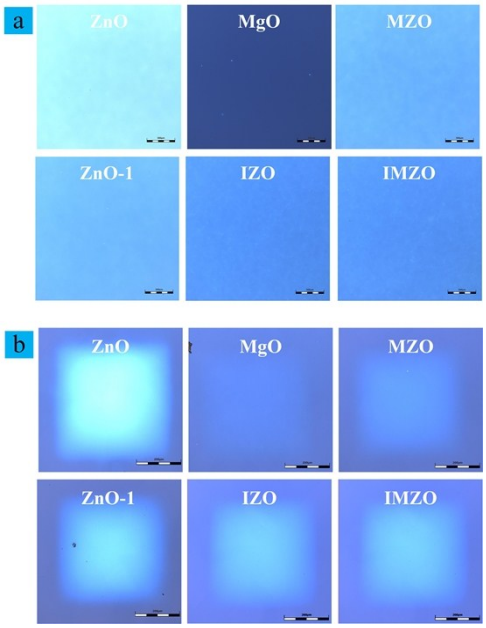

Figure S5

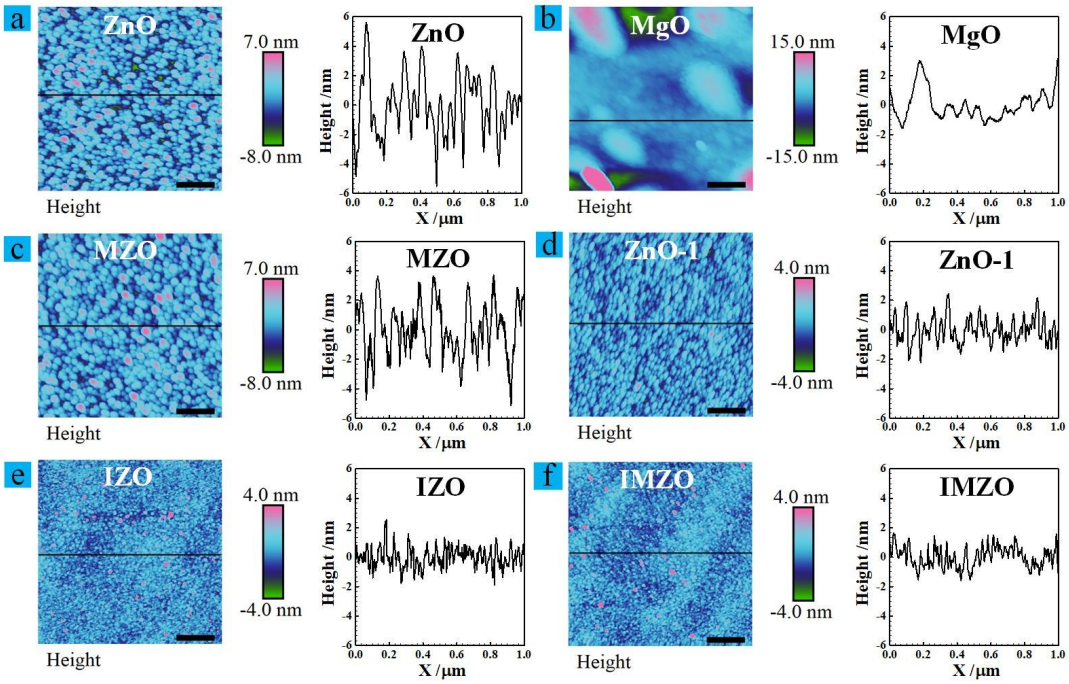
a
ZnO
7.0 nm
-8.0 nm
Height
ZnO
Height /nm
X /μm
b
MgO
15.0 nm
-15.0 nm
Height
MgO
Height /nm
X /μm
c
MZO
7.0 nm
-8.0 nm
Height
MZO
Height /nm
X /μm
d
ZnO-1
4.0 nm
-4.0 nm
Height
ZnO-1
Height /nm
X /μm
e
IZO
4.0 nm
-4.0 nm
Height
IZO
Height /nm
X /μm
f
IMZO
4.0 nm
-4.0 nm
Height
IMZO
Height /nm
X /μm

Figure S6

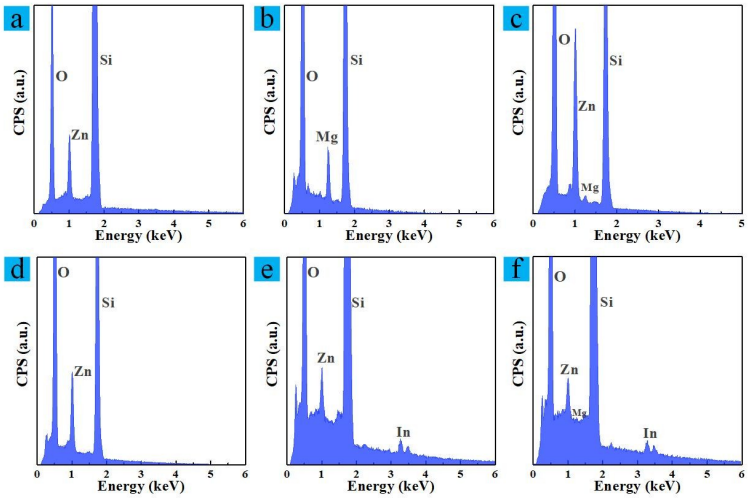

Figure S7

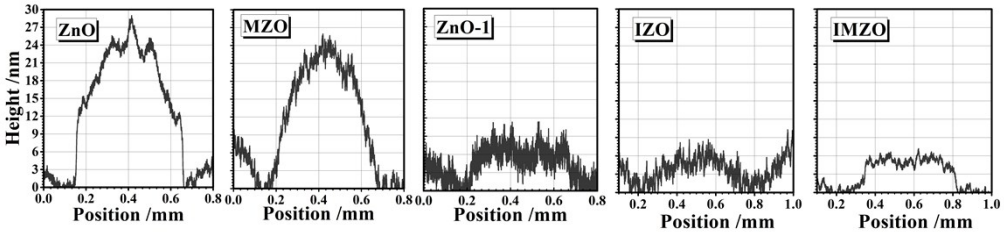

Figure S8

Table S1

Sample	I_{on}/I_{off}	μ_{FE} ($cm^2V^{-1}s^{-1}$)	μ_{FE} ($cm^2V^{-1}s^{-1}$)	I_{on} (A)	I_{on} (A)	*SS* ($V \cdot dec^{-1}$)	*SS* ($V \cdot dec^{-1}$)	V_{th} (V)	V_{th} (V)
ZnO	2.73×10^{6}	15.03	15.90	2.73×10^{-4}	2.85×10^{-4}	1.93	2.20	16	15
MZO	3.12×10^{5}	3.02	2.95	4.68×10^{-5}	4.42×10^{-5}	1.44	1.23	19	20
ZnO-1	5.57×10^{3}	0.012	0.011	1.67×10^{-7}	1.86×10^{-7}	3.66	4.17	18	18
IZO	3.60×10^{6}	14.25	16.42	3.56×10^{-4}	4.16×10^{-4}	2.09	2.04	-2	1
IMZO	7.19×10^{7}	26.67	23.74	7.24×10^{-4}	7.19×10^{-4}	0.87	0.66	-1	1

Table S2

Material	*Thickness* (nm)	*Method*	*Gate dielectric*	I_{on}/I_{off}	μ_{FE} ($cm^2V^{-1}s^{-1}$)	*SS* ($V \cdot dec^{-1}$)	V_{th} (V)	*Ref.*	*Year*
ZnO	40	Spray	HfO_2	10^7	40		6	[1]	2015
In_2O_3	6-8	Spray	AlO_X/ZrO_2	7×10^6	16		~0.4	[2]	2015
Sor/IGZO	10-11	Combustion	SiO_2	10^5−10^7	7.50		1.7	[3]	2016
IWO		Spin coating	AlO_X/SiO_2	5×10^7	15.3	0.068	2	[4]	2016
In_2O_3	10	Spray	SiO_2		38.5		-10	[5]	2017
IGZO	25	Sputtering	SiO_2	4.0×10^7	26.4	0.53	2.8	[6]	2017
IGZO	40	Sputtering	SiO_2	1.6×10^8	10.23	0.36	0.5	[7]	2018
ZnO	20	Spray	SiO_2	10^9	14.7	0.49	3.5	[8]	2019
MZO	6	Spin coating	AlO_X		4.0	0.21	2.53	[9]	2019
IMZO		Spin coating	SiO_2	2.2×10^7	1.97	0.69	-7.1	[10]	2019
InSmO	5	Spin coating	SiO_2	$>10^8$	~21.51	~0.66	~2.14	[11]	2020
IMZO	5	Spray	SiO_2	7.19×10^7	26.67	0.87	-1	This work	This work

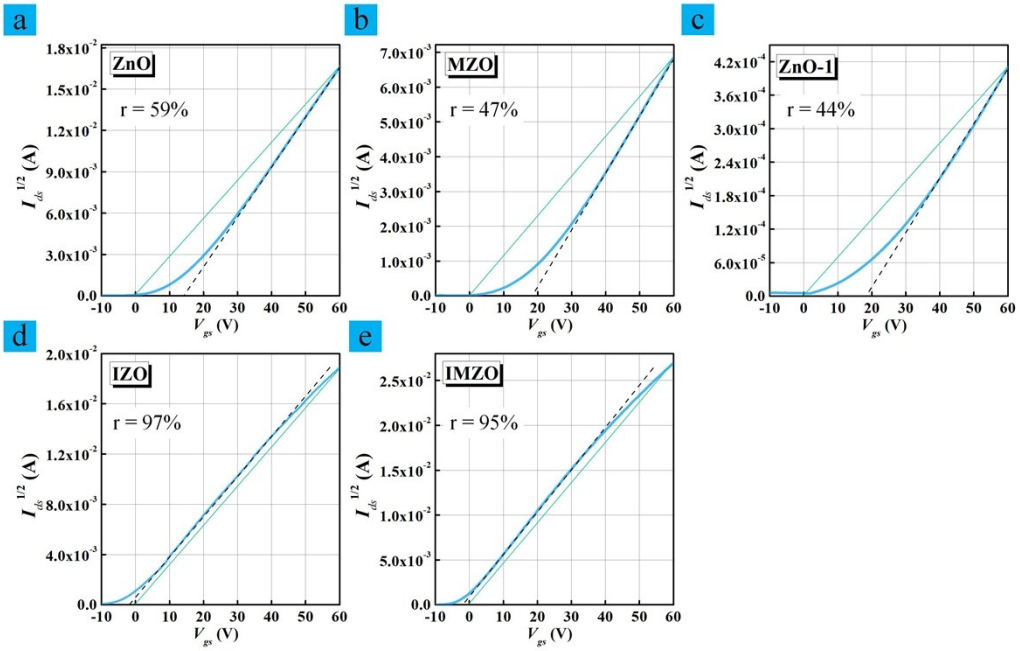

Figure S9

The reliability factor r can be expressed as **Equation S1** indicating the ratio of maximum channel conductivity from transfer characteristic data at maxiumum V_{gs} (black dashed line) to the ideal maximum conductivity (green line).

$$r = \frac{\left(\frac{\sqrt{|I_{ds}|^{\max}} - \sqrt{|I_{ds}^{0}|}}{|V_{gs}|} \right)^2}{\left(\frac{\partial \sqrt{|I_{ds}|}}{\partial V_{gs}} \right)^2} \qquad \textbf{Equation S1}$$

Where, $|I_{ds}|^{\max}$ is the drain current value at maximum V_{gs} from transfer characteristic data. $|I_{ds}|^{0}$ is the drain current value at $V_{gs} = 0$.

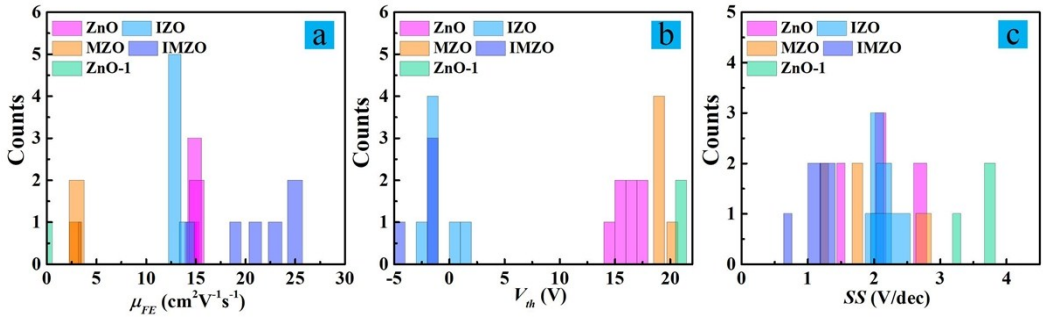

Figure S10

Table S3

Symbols (units)	*ZnO*	*MZO*	*ZnO*-1	*IZO*	*IMZO*
W (μm)	200	200	200	200	200
L (μm)	40	40	40	40	40
N_{TA} ($cm^{-3}eV^{-1}$)	9.3×10^{14}	9.3×10^{14}	9.3×10^{14}	9.3×10^{16}	9.3×10^{16}
KT_{TA} (eV)	0.05	0.05	0.05	0.05	0.05
N_{GA} ($cm^{-3}eV^{-1}$)	8.0×10^{13}	8.0×10^{13}	8.0×10^{13}	8.0×10^{13}	8.0×10^{13}
KT_{GA} (eV)	0.3	0.3	0.3	0.3	0.3
E_0 (eV)	1.7	1.7	1.7	1.7	1.7
t_{mo} (nm)	24	24	5	5	5
t_{ox} (nm)	100	100	100	100	100
V_{fb} (V)	-2.5	-1	-1.3	-7.8	-6
C_{ox} (F/cm^2)	3×10^{-8}	3×10^{-8}	3×10^{-8}	3×10^{-8}	3×10^{-8}
α (-)	0.40	0.42	0.19	0.47	0.49
β (-)	0.90	0.90	0.50	0.95	0.97
k_a (-)	40	30	0.1	30	38
k_b (-)	0.001	0.001	0.0005	0.001	0.001
a_1 (-)	0.001	0.001	0.0005	0.001	0.003
b_1 (-)	3.2	2.48	1.5	2.995	3.4

Table S4

Sample	I_{on}/I_{off}	μ_{FE} ($cm^2V^{-1}s^{-1}$)	μ_{FE} ($cm^2V^{-1}s^{-1}$)	I_{on} (A)	I_{on} (A)	*SS* ($V \cdot dec^{-1}$)	*SS* ($V \cdot dec^{-1}$)	V_{th} (V)	V_{th} (V)
IMZO-5 nm	3.76×10^{7}	22	22.92	3.76×10^{-4}	3.65×10^{-4}	0.865	0.66	-1	1
IMZO-6 nm	2.98×10^{7}	17	19.94	2.98×10^{-4}	2.92×10^{-4}	0.994	0.86	-1	3.5
IMZO-7 nm	1.19×10^{7}	12	15.65	1.19×10^{-4}	2.02×10^{-4}	0.933	0.89	2	5
IMZO-8 nm	4.23×10^{6}	3.58	3.68	4.23×10^{-5}	4.19×10^{-5}	0.877	1.39	8	7
ZnO-10nm	8.45×10^{5}	2.06	1.12	5.53×10^{-5}	1.08×10^{-5}	1.280	1.51	18	16
ZnO-21 nm	2.77×10^{6}	6.51	5.05	1.26×10^{-5}	5.21×10^{-5}	1.285	1.54	16	15
ZnO-24 nm	6.90×10^{6}	12.48	8.23	1.38×10^{-4}	8.60×10^{-5}	1.928	2.20	16	15
ZnO-35 nm	8.50×10^{6}	15.12	15.27	1.73×10^{-4}	1.95×10^{-4}	2.025	1.64	8	8

Table S5

Symbols	*IMZO* 5 nm	*IMZO* 6 nm	*IMZO* 7 nm	*IMZO* 8 nm	*ZnO* 10 nm	*ZnO* 21 nm	*ZnO* 24 nm	*ZnO* 35 nm
W (μm)	200	200	200	200	200	200	200	200
L (μm)	40	40	40	40	40	40	40	40
N_{TA} ($cm^{-3}eV^{-1}$)	9.3×10^{16}	9.3×10^{16}	9.3×10^{16}	9.3×10^{16}	9.3×10^{14}	9.3×10^{14}	9.3×10^{14}	9.3×10^{14}
KT_{TA} (eV)	0.05	0.05	0.05	0.05	0.05	0.05	0.05	0.05
N_{GA} ($cm^{-3}eV^{-1}$)	8.0×10^{13}	8.0×10^{13}	8.0×10^{13}	8.0×10^{13}	8.0×10^{13}	8.0×10^{13}	8.0×10^{13}	8.0×10^{13}
KT_{GA} (eV)	0.3	0.3	0.3	0.3	0.3	0.3	0.3	0.3
E_0 (eV)	1.7	1.7	1.7	1.7	1.7	1.7	1.7	1.7
t_{mo} (nm)	5	6	7	8	10	21	24	35
t_{ox} (nm)	100	100	100	100	100	100	100	100
$3V_{fb}$ (V)	-6	-6	-5	-4	-2.5	-2.5	-2.5	-5
C_{ox} (F/cm^2)	3×10^{-8}	3×10^{-8}	3×10^{-8}	3×10^{-8}	3×10^{-8}	3×10^{-8}	3×10^{-8}	3×10^{-8}
α (-)	0.49	0.47	0.46	0.40	0.30	0.40	0.40	0.46
β (-)	0.97	0.97	0.95	0.90	0.70	0.88	0.90	0.90
k_a (-)	38	38	38	35	30	40	40	40
k_b (-)	0.001	0.001	0.001	0.001	0.001	0.001	0.001	0.001
a_1 (-)	0.003	0.003	0.003	0.001	0.001	0.001	0.001	0.001
b_1 (-)	3.4	3.3	3.2	2.8	2.88	3.0	3.2	3.2

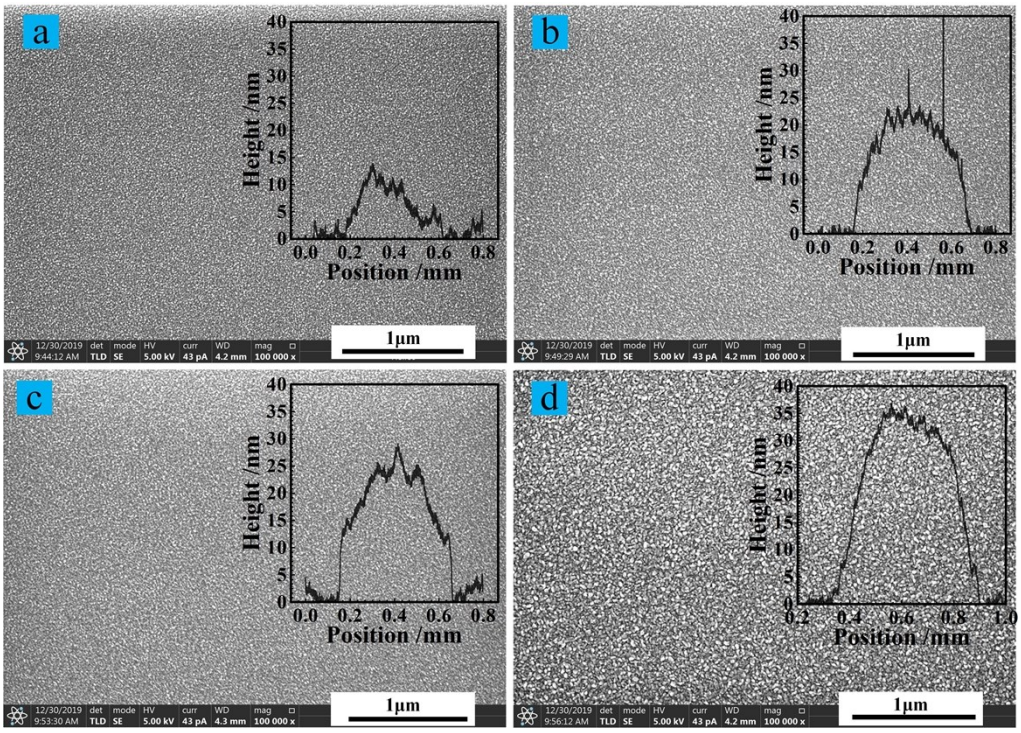

Figure S11

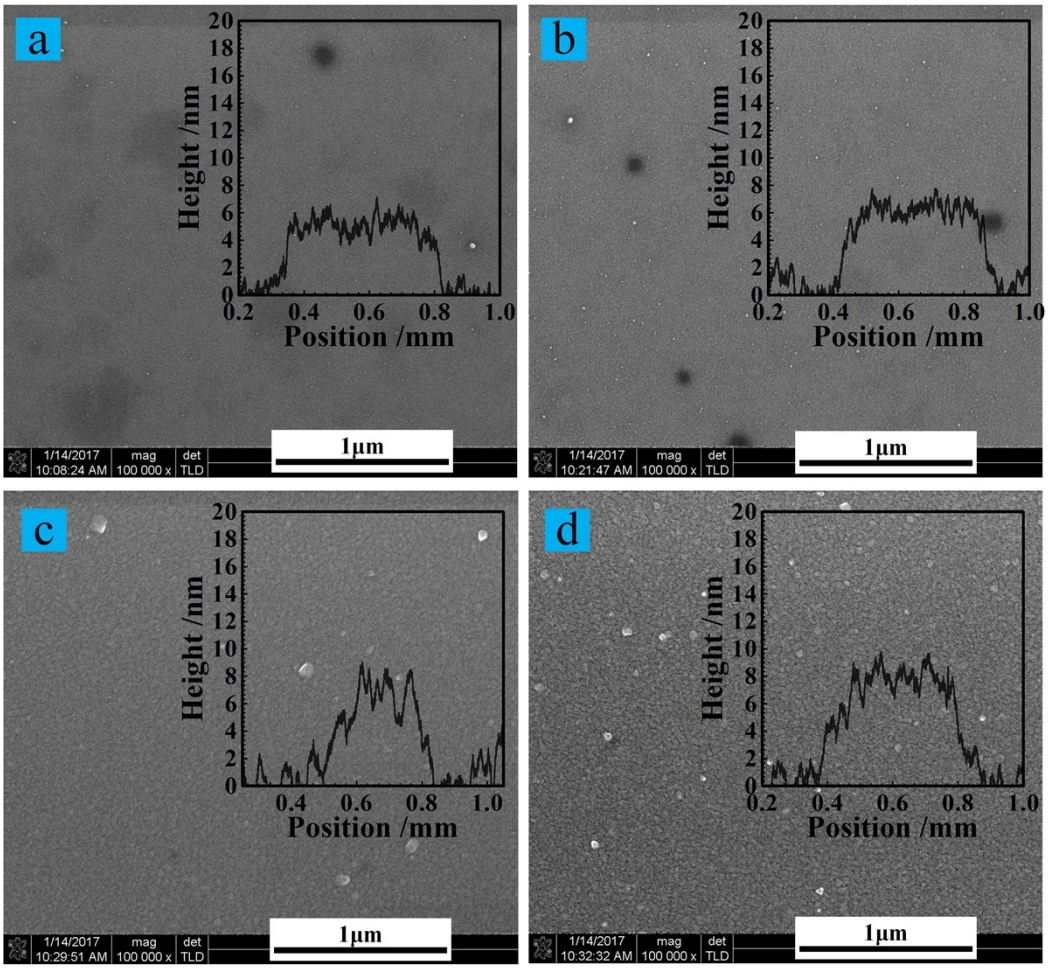
a
b
c
d
Height /nm
Position /mm
1μm
1/14/2017
10:08:24 AM
10:21:47 AM
10:29:51 AM
10:32:32 AM
mag
100 000 x
det
TLD

Figure S12

Reference

[1] M. Esro, G. Vourlias, C. Somerton, W. I. Milne, G. Adamopoulos, High-Mobility ZnO Thin Film Transistors Based on Solution-processed Hafnium Oxide Gate Dielectrics. **Advanced Functional Materials**, **2015**, **25**(1): 134-141.

[2] H. Faber, Y. H. Lin, S. R. Thomas, K. Zhao, N. Pliatsikas, M. A. McLachlan, A. Amassian, P. A. Patsalas, T. D. Anthopoulos, Indium Oxide Thin-Film Transistors Processed at Low Temperature via Ultrasonic Spray Pyrolysis. **ACS Applied Materials & Interfaces**, **2015**, **7**(1): 782-790.

[3] Binghao Wang, Li Zeng, Wei Huang, Ferdinand S. Melkonyan, William C. Sheets, Lifeng Chi, Michael J. Bedzyk, Tobin J. Marks, Antonio Facchetti, Carbohydrate-Assisted Combustion Synthesis To Realize High-Performance Oxide Transistors. **Journal of the American Chemical Society**, **2016**, **138**(22): 7067-7074.

[4] Ao Liu, Guoxia Liu, Huihui Zhu, Byoungchul Shin, Elvira Fortunato, Rodrigo Martins, Fukai Shan, Eco-friendly, solution-processed In-W-O thin films and their applications in low-voltage, high-performance transistors. **Journal of Materials Chemistry C**, **2016**, **4**(20): 4478-4484.

[5] Ivan Isakov, Hendrik Faber, Max Grell, Gwenhivir Wyatt-Moon, Nikos Pliatsikas, Thomas Kehagias, George P. Dimitrakopulos, Panos P. Patsalas, Ruipeng Li, Thomas D. Anthopoulos, Exploring the Leidenfrost Effect for the Deposition of High-Quality In2O3 Layers via Spray Pyrolysis at Low Temperatures and Their Application in High Electron Mobility Transistors. **Advanced Functional Materials**, **2017**, **27**(22): 1606407.

[6] Ablat Abliz, Qingguo Gao, Da Wan, Xingqiang Liu, Lei Xu, Chuansheng Liu, Changzhong Jiang, Xuefei Li, Huipeng Chen, Tailiang Guo, Jinchai Li, Lei Liao, Effects of Nitrogen and Hydrogen Codoping on the Electrical Performance and Reliability of InGaZnO Thin-Film Transistors. **ACS Applied Materials & Interfaces**, **2017**, **9**(12): 10798-10804.

[7] Hyukjoon Yoo, Young Jun Tak, Won-Gi Kim, Yeong-gyu Kim, Hyun Jae Kim, A selectively processible instant glue passivation layer for indium gallium zinc oxide thin-film transistors fabricated at low temperature. **Journal of Materials Chemistry C**, **2018**, **6**(23): 6187-6193.

[8] Junhee Cho, Seongkwon Hwang, Doo-Hyun Ko, Seungjun Chung, Transparent ZnO Thin-Film Deposition by Spray Pyrolysis for High-Performance Metal-Oxide Field-Effect Transistors. **Materials**, **2019**, **12**(20): 3423.

[9] Jae Sang Heo, Seong-Pil Jeon, Insoo Kim, Woobin Lee, Yong-Hoon Kim, Sung Kyu Park, Suppression of Interfacial Disorders in Solution-Processed Metal Oxide Thin-Film Transistors by Mg Doping. **ACS Applied Materials & Interfaces**, **2019**, **11**(51): 48054-48061.

[10] Jin Cheng, Xuyang Li, Jian Guo, Haifei Xu, Yonghua Chen, Yunfei He, Jianshe Xue, Ting Zhang, Zhinong Yu, The role of the sequence of plasma treatment and high temperature annealing on solution-processed a-IMZO thin film transistor. **Journal of Alloys and Compounds**, **2019**, **793**: 369-374.

[11] Yanwei Li, Deliang Zhu, Wangying Xu, Shun Han, Ming Fang, Wenjun Liu, Peijiang Cao, Youming Lu, High-mobility nanometer-thick crystalline In–Sm–O thin-

film transistors via aqueous solution processing. **Journal of Materials Chemistry C**, **2020**, **8**(1): 310-318.